SAGE CRISP PUBLICATIONS DIRECTORY

Authors:-

Watson, G.V.R. and Carder, D.R.

COMPARISON OF THE MEASURED AND COMPUTED PERFORMANCE OF A PROPPED BORED PILE RETAINING WALL AT WALTHAMSTOW

Publication:-

PROC. INST. OF CIVIL ENGINEERS, GEOTECHNICAL ENG., 107, pp 127-133

Year of Publication:-

1994

Comparison of the measured and computed performance of a propped bored pile retaining wall at Walthamstow

G. V. R. Watson and D. R. Carder

Proc. Instn Civ. Engrs Geotech. Engng, 1994, **107**, July, 127–133

Ground Board

Geotechnical Engineering Advisory Panel Paper 10447

Written discussion closes 15 September 1994

This Paper compares the results of field monitoring during the construction of a bored pile retaining wall propped at carriageway level with the computed results from finite element analyses using the Mohr-Coulomb model. Field monitoring was carried out to measure ground movements, total lateral stresses and porewater pressures, together with wall movements and bending moments. Generally, good correlation was obtained between the measured and computed results.

This analysis was performed as a back analysis but all the data used was available prior to construction and could therefore have been used in a class A prediction.

Introduction

Many deep excavations for road improvement schemes in urban areas are currently being constructed using bored pile and diaphragm retaining walls. This is particularly so in the London area, where site access and availability of land make other engineering solutions less viable. The structural loading on walls and movements in the nearby ground will depend upon the stiffness of the wall, the type of support system, the initial stress state in the ground and the stress changes occurring during each construction stage (see Potts and Fourie[1] and Higgins, Potts and Symons[2]).

2. Comprehensive instrumentation was installed at Walthamstow on the A406, North Circular Road in London, to monitor soil-structure interaction during the construction of a contiguous bored pile wall founded in London Clay. At this site, excavation in front of the walls took place beneath temporary props which spanned the underpass with the finished structure being permanently propped below the carriageway using a hinged design at the prop–wall connection. At the instrumented section, the wall was formed from 17 m long, 1·5 m dia. piles at 1·7 m centres with a retained height of 8 m. Other dimensions are shown in Fig. 1. The results and interpretation of the site data are reported by Carswell, Carder and Gent.[3]

3. In this Paper the site observations have been compared with the results from finite element analyses.

Basis of analyses

4. The finite element analyses were performed using the CRISP90 package (Britto and Gunn).[4] The soil was modelled as an elastic perfectly plastic material with the yield surface being defined by the Mohr-Coulomb yield criterion.

5. Initially, an axisymmetric analysis was carried out to simulate the installation of a single pile by removing soil elements and replacing them with concrete elements at the axis of rotation. As pile installation on site took place very quickly over a period of a few hours, undrained conditions were assumed for this analysis.

6. A more detailed mesh was constructed to accommodate the different soil strata and also to enable the underpass construction sequence to be modelled by removal of elements. This analysis was carried out under plane strain conditions with the wall being 'wished in-place' and a coupled consolidation analysis performed to model the long term condition.

Material properties

Soil parameters

7. The soil properties used in the analyses came from several sources, the original site investigations carried out in August 1983 and January 1988 together with TRL in-situ testing carried out in May 1992 at an adjacent 'green field' site. The rest of the material properties were drawn from previous analyses in London Clay (see Burland and Kalra[5] and Carswell, Carder and Symons[6]).

8. The soil strata profile was developed from the 1983 site investigation. This gave best fit strength parameters of $c' = 20$ kNm^{-2} and $\phi' = 22°$ for the London Clay, and these values were used for the Mohr-Coulomb analyses. Following the upper bound recommended by Burland and Kalra,[5] the clay modulus was varied with depth using

$$E' = 32 + 8{\cdot}4z \qquad (1)$$

where E' is the drained elastic modulus in MNm^{-2} and z is the depth in metres.

Geoff Watson, Higher Scientific Officer, Bridges & Ground Engineering Resource Centre, Transport Research Laboratory, Crowthorne

Derek Carder, Principal Scientific Officer, Bridges & Ground Engineering Resource Centre, Transport Research Laboratory, Crowthorne

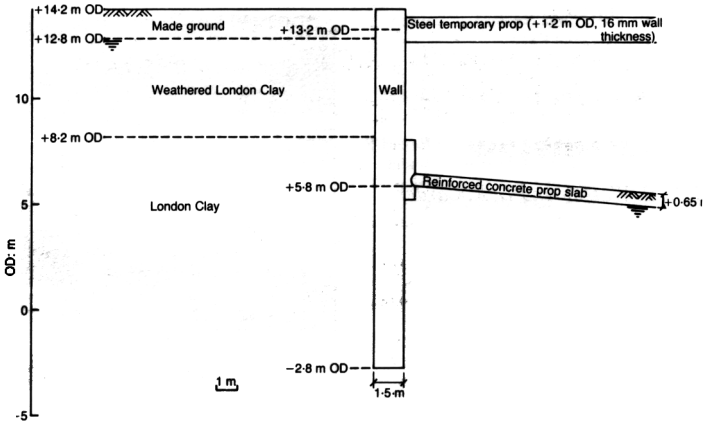

Fig. 1. Cross-section

9. The equivalent values of shear modulus $G_u\{=G'=E'/[2(1+\upsilon')]\}$ calculated using equation (1) and a Poisson's ratio υ' of 0·2 agreed well with the upper bound values from reload loops measured by TRL using the self-boring pressuremeter. The modulus of the 1·4 m layer of made ground was taken as 10 MNm^{-2}. The soil parameters are summarized in Table 1.

10. The initial value of K (the ratio of horizontal to vertical effective stress) in the clay was taken as 2 from self-boring pressuremeter and Marchetti dilatometer testing carried out by TRL in the adjacent green field site (see Carswell *et al.*).[3] Piezometer measurements indicated that the water-table was approximately hydrostatic from the clay surface prior to construction. During construction perforated plastic drainage ducts were installed between each of the piles and connected to the underpass drainage system. For this reason, in the coupled consolidation analysis, the absolute pore-water pressure was forced to zero over both the retained part of the wall and immediately beneath the base of the prop slab. Horizontal and vertical permeabilities of 5×10^{-10} m/sec and 1×10^{-10} m/sec were assumed for the clay. These values are similar to those measured in situ by Burland and Hancock[7] with some allowance being made for anisotropy in the London Clay.

Table 1. Soil parameters used in finite element analyses

Soil type	Depth: m	c': kNm^{-2}	ϕ'	Poisson's ratio, υ'	Bulk density: kNm^{-3}
Made ground	0–1·4	0	30°	0·2	18
Weathered London Clay	1·4–6	20	22°	0·2	19·1
Unweathered London Clay	6–40	20	22°	0·2	19·9

Structural components

11. In the analyses, three main structural elements were used to represent the bored pile wall, the temporary props and the permanent prop slab. The wall comprised 17 m deep, 1·5 m dia. piles at 1·7 m centres with a pile flexural stiffness of $7·6 \times 10^6$ kNm^2. This was modelled using a 1·5 m thick wall of unit length in the plane strain analysis giving an equivalent stiffness E of $1·6 \times 10^7$ kNm^{-2} per metre run of the wall. These values were calculated using a concrete stiffness of $2·6 \times 10^7$ kNm^{-2} and assuming that the concrete remained uncracked at the small strain levels involved. It must be noted that lower values might be used in long term design in order to allow for cracking and creep of the concrete (see Powrie and Li).[8]

12. The steel temporary props were 1·2 m dia. at 2·7 m centres and were grouted in position at 1·25 m depth below the original ground level. These were modelled using rectangular elements with equivalent stiffness and density of 4×10^3 kNm^{-2} and 1·45 kNm^{-3}.

13. The permanent prop slab was 0·65 m thick reinforced concrete constructed with a shallow V-shaped profile dipping towards the centre (see Fig. 2). For the analysis, this was assumed to be symmetrical about the centreline of the underpass, although in reality it was slightly asymmetric. The connection between the wall and the slab was hinged (Carswell *et al.*)[3] and for this reason was modelled as a pin joint connection (see Powrie and Li)[8] to allow the wall to rotate about the prop. A stiffness E

of 3×10^7 kNm^{-2} was assumed for the reinforced concrete prop slab.

Modelling of construction sequence

Pile installation

14. The axisymmetric run was performed to provide an assessment of the movement and stress relief caused by the installation of a single bored pile. As individual piles were installed very rapidly on site, and generally no two adjacent piles were constructed on the same day, the approach was considered a reasonable compromise with a more rigorous three-dimensional approach being considered unnecessary. An alternative approach (see Higgins *et al.*)[2] would have been to model wall installation using the plane strain mesh, but this would have assumed excavation of an infinitely long wall and provided an upper bound solution. As previously mentioned, this analysis was performed under undrained conditions.

Underpass construction and long term performance

15. The following stages of underpass construction were modelled

(*a*) initial excavation to 1·4 m depth in front of the wall to provide access for temporary propping
(*b*) period (100 days) between initial excavation and installation of temporary props
(*c*) installation of temporary props and excavation to 6 m depth over a period of 10 days
(*d*) excavation to 7·9 m over a period of 12 days
(*e*) excavation to full depth of 8·4 m over a period of 18 days
(*f*) period (47 days) between excavation and pouring of permanent prop
(*g*) permanent prop slab cast
(*h*) temporary props removed
(*i*) consolidation over a period of 120 years.

16. Although a coupled consolidation model was used throughout the analysis of underpass construction and service life, a separate undrained analysis up to the end of bulk excavation was found to give almost identical results.

Results and discussion

17. The results from the analyses have been compared with field measurements reported by Carswell *et al.*[3] for the construction period and the first six months after opening of the underpass to traffic. Measurements are still ongoing at the site which should enable a more detailed comparison to be made between long term performance and predictions.

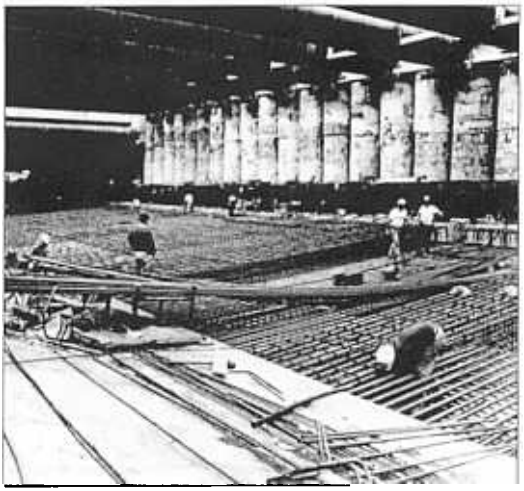

Fig. 2. Temporary props and construction of permanent prop slab

18. As was expected, the axisymmetric model of an individual pile installation gave smaller ground movements than were observed on site during wall installation. A maximum lateral movement of 1 mm was predicted at 1·1 m away on the ground surface during installation of a single pile; this value can be compared with that of 3 mm measured during installation of the row of piles forming the wall in the instrumented area. Both the observed and numerical results confirmed that there was comparatively little ground movement and consequently only a minimal amount of lateral stress relief (<10%) during the wall installation phase of construction. No further account was therefore taken of the effects of wall installation in the modelling of underpass construction at this particular site, although it should be noted that embedded wall installation effects at other sites have been far more significant (see Symons and Carder).[9]

19. Figure 3 shows the predicted lateral wall movements at various stages in the construction and those determined on site using inclinometer and Geomensor electronic distance measurements. The general trends in both sets of data were very similar with predicted movements at the ground surface being within about 2 mm of those measured. However, the finite element model indicated a forward movement of the wall toe of about 8 mm whereas a small backward movement of less than 2 mm was actually recorded on site. Similar behaviour was observed by Symons *et al.*[10] at Bell Common Tunnel, where analyses also over-

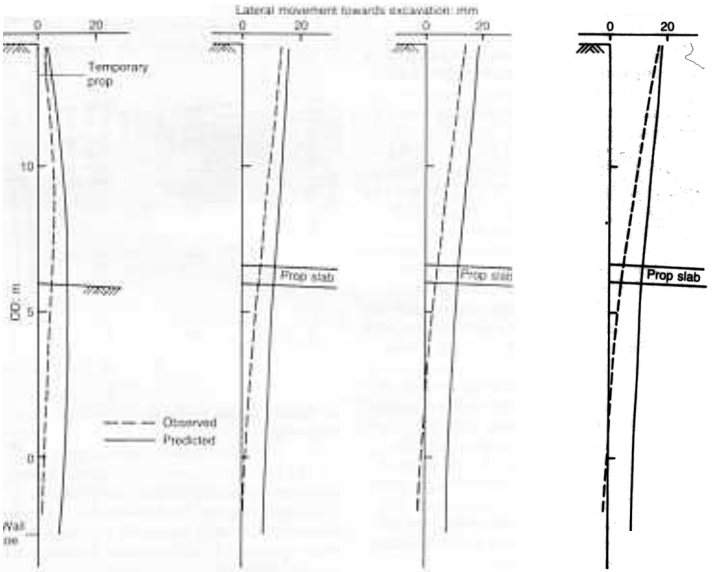

Fig. 3. Lateral wall movements developed during construction

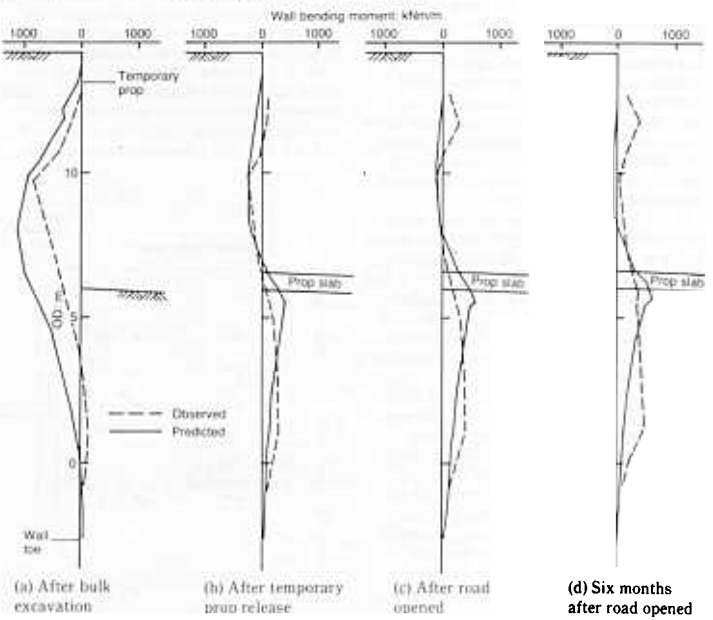

Fig. 4. Wall bending moments developed during construction

predicted movements of the toe of the secant pile retaining walls.

20. The predicted bending moments in the wall are compared with those determined using vibrating wire strain gauges mounted on the steel reinforcing cage in pairs at the front and back. In evaluating moment, bending strain ε_b was first calculated at each depth from $\frac{1}{2}(\varepsilon_1 - \varepsilon_2)$, where ε_1 and ε_2 are the strains on the front and back of the wall. Bending moment is then given by $EI(d^2y/dx^2)$, i.e. $EI\varepsilon_b/c$ where c is equal to the pile radius. The comparison of these results is shown in Fig. 4. Immediately after excavation to formation level, the analysis gave a peak bending moment of 1100 kNm per metre run of wall compared with a measured moment of 850 kNm. However, the analysis predicted the peak at 6 m below ground level while the field measurements indicated a maximum at about 4·5 m below ground level. The predicted temporary prop load at this stage was 455 kN per metre run of wall and this can be compared with measured values varying between 200 kN and 480 kN depending on temperature. The thermal expansion effects with steel props of this type are well known and as such the props provide proactive support (see Fernie).[11] The predicted and measured bending moment profiles shown in Fig. 4 remained broadly similar at later stages of construction.

21. Figure 5 shows ground movement vectors and horizontal wall movement at six months after road opening. In general, the finite element analysis tended to slightly over-predict lateral movement and under-predict settlement. Lateral movement was particularly well predicted close to the wall on the retained side, while some overestimation occurred further back. Reduced ground movements further away would probably have been predicted if a more sophisticated soil model had been employed with increased soil stiffness at low strain (see Higgins *et al.*[2] and Simpson[12]).

22. The predicted ground and wall movements after approximately 120 years are shown in Fig. 6. Little change in the lateral movements was determined from those reported in Fig. 5 at six months after opening of the road to traffic. Generally, more heave was calculated for this period particularly in front of the wall where some dissipation of negative excess pore-water pressure was still occurring.

23. Figure 7 shows the total lateral stress distributions determined from both field measurements and the finite element analysis immediately after opening the road to traffic. Generally, the analysis predicted slightly higher stresses on the retained side at depth than were measured. On the excavated side reasonable agreement was obtained although there was some indication from the spade pressure cell at about 3 m below formation level that higher stresses may be developing at shallow depths below the permanent prop slab.

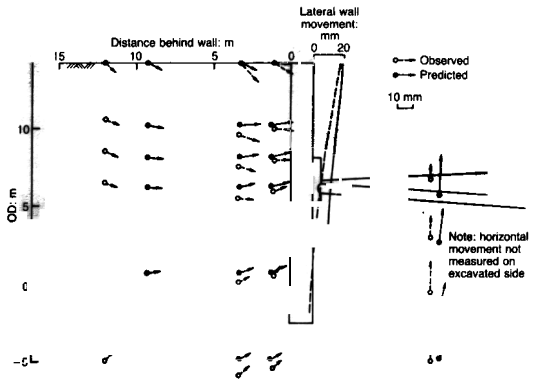

Fig. 5. Ground and wall movements six months after road opened

24. The finite element stresses, calculated for 120 years after construction, are compared with values typically used in design in Fig. 8. Close to the wall on the retained side, the total lateral stresses were compared with those corresponding to a K value of unity. Although K is an effective stress ratio, when its value is unity the total lateral stress equals the overburden stress and is independent of the pore-water pressure distribution. On the excavated side, effective stresses were calculated using the best fit soil parameters from triaxial compression tests of $c' = 20\ kNm^{-2}$ and $\phi' = 22°$, and lower bound values of $c' = 0$ and $\phi' = 22°$. The values of passive earth pressure coefficient K_p were determined assuming a wall friction angle of $\phi'/2$ and zero wall cohesion from Caquot and

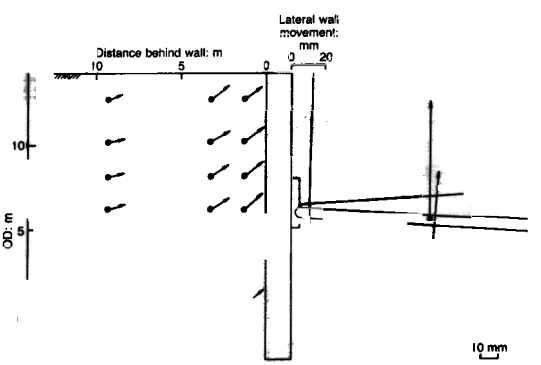

Fig. 6. Predicted ground and wall movements after . years

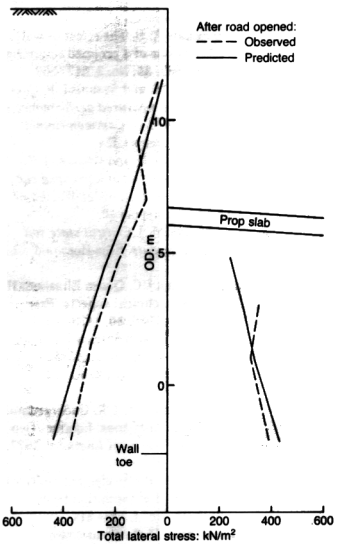

Fig. 7. Total lateral stress distributions at 1·1 m from the wall faces

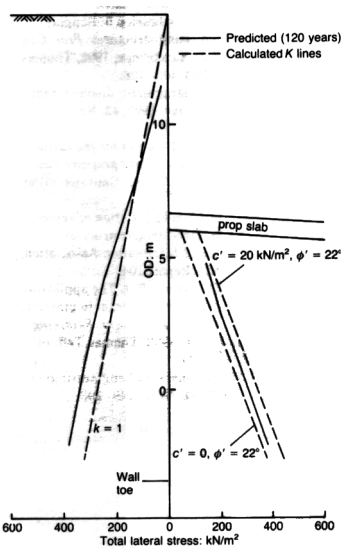

Fig. 8. Comparison of predicted lateral stresses with typical values used in design

Kerisel[13] in accordance with the recommendations of Padfield and Mair.[14] Total stresses were then calculated from these effective stresses by using the design assumption of a hydrostatic distribution of pore-water pressure with depth. This latter assumption was substantiated by the post-construction pore-water pressure data reported by Carswell *et al.*[3] The total lateral stresses from the finite element analysis fell between the design values calculated in this way (see Fig. 8).

25. Pore-water pressure distributions (Fig. 9) showed reasonable correlation between the analysis and the observations on the retained side but not on the excavated side. The analysis suggested that negative excess pore-water pressures still existed in this area as a consequence of bulk excavation, whereas the limited experimental evidence from the two piezometers installed in front of the wall indicated that significant pore-water pressure dissipation had already occurred. This discrepancy probably occurred because the analysis was carried out assuming plane strain conditions with the wall behaving in an impermeable manner. In reality the piles forming the wall are contiguous (1·5 m piles at 1·7 m centres), seepage through the wall will therefore result in faster pore-water pressure dissipation than that predicted. This same point could account for the higher total stresses measured at shallow depths in front of the wall after the road was opened.

26. Both measured and predicted loads in the permanent prop slab at carriageway level were about 500 kN per metre run of wall when the road was opened to traffic. Subsequent measurements have shown a further increase in load after this time, with a seasonal variation as the permanent prop expanded and contracted with temperature. A maximum load of about 1500 kN per metre run was measured in summer and a minimum load of about 1000 kN in winter. The finite element analysis predicted a slow increase in permanent prop load to a value of 675 kN at 120 years, although the thermal effects of prop slab expansion were not modelled.

Conclusions

27. When using finite elements in the design of embedded retaining walls, validation against real problems is required (see Woods and Clayton).[15] In this case history study of the performance of a propped bored pile wall founded in stiff clay at Walthamstow, good correlation was obtained between finite element analysis based on the Mohr-Coulomb model and the field measurements. Although the analytical work was not a true class A prediction (see Lambe)[16] in so far as it was performed as a back-analysis after construction, all the parameters (including the in situ stress regime) were

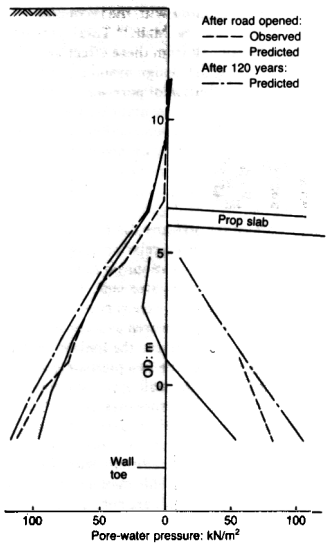

Fig. 9. Pore-water pressure distributions at 1·1 m from the wall faces

available from the site investigation and in situ testing carried out prior to construction. Close modelling of the temporary and permanent propping systems and the construction sequence were considered to be of paramount importance in obtaining a realistic prediction of behaviour.

Acknowledgements

28. The work described in this Paper forms part of the research programme of the Bridges and Ground Engineering Resource Centre of TRL and is published by permission of the Chief Executive. The study was funded by Bridges Engineering Division of the Department of Transport. Aspects of the field work reported separately were part funded by Cementation Construction Ltd and Bullen and Partners Consulting Engineers. The views expressed in this paper are not necessarily those of the Department of Transport.

References

1. POTTS D. M. and FOURIE A. B. The effect of wall stiffness on the behaviour of a propped retaining wall. *Géotechnique*, 1985, **35**, No. 3, 347–352.
2. HIGGINS K. G., POTTS D. M. and SYMONS I. F. *Comparison of predicted and measured performance of the retaining walls of the Bell Common tunnel.* 1989, TRRL Contractor Report 124.
3. CARSWELL I. G., CARDER D. R. and GENT A. J. C. *Behaviour during construction of a propped contiguous bored pile wall in stiff clay at Waltham-stow.* 1993, TRL Project Report 10.
4. BRITTO A. M. and GUNN M. J. *Critical state soil mechanics via finite elements.* Ellis Horwood, Chichester, 1987.
5. BURLAND J. B. and KALRA J. C. Queen Elizabeth II Conference Centre: geotechnical aspects. *Proc. Instn Civ. Engrs*, Part 1, 1986, **80**, 1479–1503.
6. CARSWELL I., CARDER D. R. and SYMONS I. F. *Long term performance of an anchored diaphragm wall embedded in stiff clay.* 1991, TRL Research Report 313.
7. BURLAND J. B. and HANCOCK R. J. R. Underground car park at the House of Commons, London: Geotechnical aspects. *The Structural Engineer*, 1977, **55**, No. 2, 87–100.
8. POWRIE W. and LI E. S. F. Finite element analyses of an in situ wall propped at formation level. *Géotechnique*, 1991, **41**, No. 4, 499–514.
9. SYMONS I. F. and CARDER D. R. Stress changes in stiff clay caused by the installation of embedded retaining walls. *Proc. Conf. Retaining Structures*, Cambridge, 1992, Thomas Telford, London, 1993, 227–236.
10. SYMONS I. F., POTTS D. M. and CHARLES J. A. Predicted and measured behaviour of a proposed embedded retaining wall in stiff clay. *Proc. 11th ICSMFE, San Francisco.* A. A. Balkema, Rotterdam, Netherlands, 1985, 2265–2268.
11. FERNIE R. Introduction to session 5: Support systems to earth retaining structures. *Proc. Conf. Retaining Structures*, Cambridge, 1992, Thomas Telford, London, 1993, 403–408.
12. SIMPSON B. Retaining structures: displacement and design. *Géotechnique*, 1992, **42**, No. 4, 541–576.
13. CAQUOT A. and KERISEL J. *Tables for the calculation of passive pressure, active pressure and bearing capacity of foundations.* Gauthier-Villars, Paris, 1948.
14. PADFIELD C. G. and MAIR R. J. *Design of retaining walls embedded in stiff clay.* Construction Industry Research and Information Association, London, 1984, CIRIA Report 104.
15. WOODS R. I. and CLAYTON C. R. I. The application of the CRISP finite element program to practical retaining wall problems. *Proc. Conf. Retaining Structures*, Cambridge, 1992, Thomas Telford, London, 1993, 102–111.
16. LAMBE T. W. Predictions in soil engineering. *Géotechnique*, 1973, **23**, No. 2, 149–202.